JUNE, 2025

Textile Sciences and Engineering

Editor
Assist. Prof. Mustafa Konuk, Ph.D.

DOI: 10.5281/zenodo.15772820

Textile Sciences and Engineering

Editor

Assist. Prof. Mustafa Konuk, Ph.D.

Publisher
Platanus Publishing®

Editor in Chief
Assist Prof. Mustafa Konuk, Ph.D.

Cover & Interior Design
Platanus Publishing®

The First Edition
June, 2025

ISBN

978-625-7609-00-5

Platanus Publishing®
Address: Natoyolu Cad. Fahri Korutürk Mah. 157/B, 06480, Mamak, Ankara, Turkey.

Phone: +90 312 390 1 118
web: www.platanuspublishing.com
e-mail: platanuskitap@gmail.com

Platanus Publishing®

CONTENTS

CHAPTER 1 5

Thermo-Oxidative Stabilization-Induced Structural Transformations in Hemp Fibers for Eco-Friendly Activated Carbon Fiber Production

Abdullah Gül & Ismail Tiyek & Kemal Şahin Tunçel & Nesrin Korkmaz

CHAPTER 2 29

Some Structural Characterizations of Nanofibers Obtained by Electrospinning Method for the Production of Environmentally Friendly Membrane with Industrial Hemp Additives

Abdullah Gül & Ismail Tiyek & Ahmet Karadağ & İbrahim Kılıç

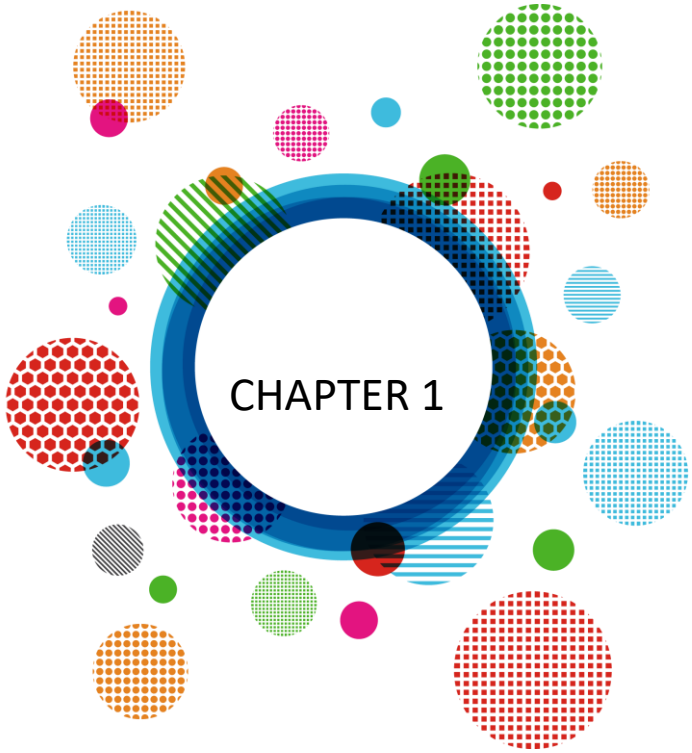

Thermo-Oxidative Stabilization-Induced Structural Transformations in Hemp Fibers for Eco-Friendly Activated Carbon Fiber Production

Abdullah Gül[1] & Ismail Tiyek[2] & Kemal Şahin Tunçel[3] & Nesrin Korkmaz[4]

[1] Dr. Öğr. Üyesi, Hemp Research Institute, Yozgat Bozok University, Yozgat, 66100, Turkey, ORCID ID: 0000-0001-6990-417X, Correspondence to
[2] Doç. Dr., The Department of Textile Engineering, Kahramanmaraş Sutcu Imam University, Kahramanmaraş, 46100, Turkey, ORCID ID: 0000-0002-1643-8977
[3] Dr. Öğr. Üyesi, Department of Traditional Crafts, Siirt University, Siirt, 56100, Turkey ORCID ID: 0000-0001-5095-6543
[4] Doç. Dr. Hemp Research Institute, Yozgat Bozok University, Yozgat, 66100, Turkey ORCID ID: 0000-0002-7896-1042

Introduction

Due to their durability, low weight, and excellent heat resistance combined with their high specific hardness, carbon fibers are widely used as reinforcement material for composites applied in wind turbine blades, automotive industries, aerospace, and civil engineering (Bengtsson et al. 2022; Liu et al. 2019). In addition, it is one of the most commonly used reinforcement elements in the preparation of high-performance composites has become one. These fibers contain more than 90% carbon in their chemical structure (Karacan and Gül 2014).

It is one of the most commonly used the biggest obstacle to the limited industrial application areas of carbon fibers is their high production costs. As a carbon fiber precursor material, polyacrylonitrile (PAN) holds significant importance in industrial applications. The manufacturing process of PAN, which is a fossil-based polymer and accounts for approximately 96% of the total production of carbon fibers, is expensive and accounts for approximately half of the cost, resulting in high prices due to its energy-intensive production process. This prevents the use of carbon fibers in wider applications (Newcomb 2016; Baker and Rials 2013).

The first known carbon fiber was produced by Thomas Alva Edison from cellulosic raw materials to be used as filaments in electric light bulbs. The carbon fiber discovered by Edison; from cellulose-based materials such as cotton or bamboo has been made and it is not fossil fuel-based like today (Edison 1880; Bortner 2003). Most carbon fibers are manufactured from precursor materials derived from fossil fuels. Given the finite availability of these resources and the scarcity of renewable alternatives, enhancing and advancing production methods has become essential. Consequently, exploring affordable and sustainable precursor materials for carbon fibers has emerged as a critical priority. In recent years, scientific research has focused on various natural sources capable of being transformed into high-performance carbon fibers. Among the cellulose-based materials utilized for this purpose are viscose rayon (Karacan and Soy 2013a, b), sisal (Fu 2003), bamboo, jute (Rahman and Karacan 2022a), cotton stalk (Li et al. 2011), and flax (Rahman and Karacan 2022b). Nevertheless, limited research has been conducted on hemp fibers as a potential raw material for producing activated carbon fiber (Williams and Reed 2004; Rosas et al. 2009).

Hemp fiber is one of the most useful plants known for its biomass production. Sometimes it may need moderate or sometimes no water and fertilizer requirements. Industrial hemp is highly advantageous as it thrives in diverse climates and locations with minimal reliance on pesticides, making it an eco-friendly and sustainable fiber source. Extracted from the phloem layer of hemp stems, bast fibers demonstrate the following chemical composition: cellulose (65-

77%), hemicellulose (7-20%), pectin (0.7-2.2%), lignin (3-6%), water-soluble compounds (0.6-1.6%), and waxes (0.8-1.8%). The cellulose within this structure exists in both amorphous and crystalline phases (Borsa et al. 2016), while lignin and hemicellulose exhibit amorphous molecular configurations (Kabir et al. 2013).

Lignin, with a carbon content of around 60–65%, is considered the most viable alternative to petroleum-based PAN precursors in carbon fiber production due to its high carbon yield potential (Bengtsson et al. 2019). Cellulose, being the dominant component in industrial hemp fibers, is a promising candidate for carbon-based fiber production. Unlike some materials, cellulose decomposes thermally without melting and possesses a tightly packed crystalline structure. During thermal oxidative stabilization, the hydroxyl groups in cellulose facilitate the formation of both intramolecular and intermolecular hydrogen bonds.These bonds can quickly form crystal structures (Dumanlı and Windle 2012). In the published literature, the use of cellulose alone (Il et al. 2016; Fukuzumi et al. 2010) and also in combination with lignin (Bengtsson et al 2019; Byrne et al. 2018) has been reported for this goal. Lignin is an amorphous, high molecular weight macromolecule composed of polyaromatic structures. In its natural form, it contains phenylpropane units with hydroxyl, methoxyl, and carbonyl functional groups (Gregorová et al. 2006; Lu et al. 2017; Huang 2009).

The theoretical carbonization efficiency of raw cellulose is 44.4%. It has been reported in studies that the experimental value is very low. Research indicates this value fluctuates from 10% to 30%, with dependence on four key parameters: the precursor fiber's structure, heating rate, processing atmosphere, and temperature (Bengtsson et al., 2019; Chand, 2000). Depolymerization of cellulose chains results in the formation of carbon monoxide, carbon dioxide, aldehydes, organic acids and tars during heat treatment, which is the reason for the low carbonation efficiency (Poovaiah et al. 2014). During pyrolysis, the depolymerization of cellulose causes a large weight decline throughout the production of volatiles. The production of activated carbon fiber involves multiple sequential steps. Initially, the precursor material may undergo chemical impregnation as an optional pretreatment. This is followed by thermal-oxidative stabilization, carbonization, and finally activation, all conducted under oxygen-free conditions (Fig. 1).

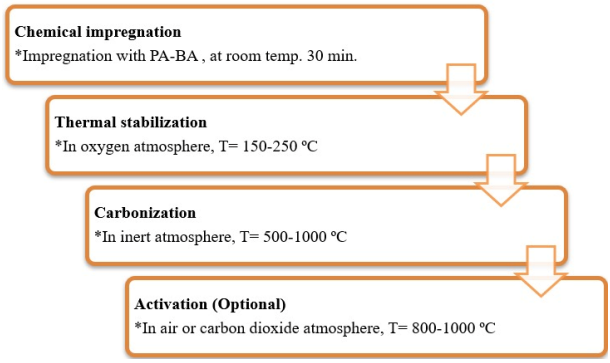

Fig. 1 Process flowchart for producing activated carbon fiber from hemp

Thermal stabilization is a critical stage that has a direct effect on the microstructure and strength structures of the last production fibers. The thermal oxidative stabilization process serves to structurally prepare precursor fibers for subsequent high-temperature treatment ranging from 500°C to 1500°C. The thermal stabilization process in the air medium is generally carried out by heat treatments up to 300°C. Where intramolecular cyclization, intermolecular cross-linking, oxidation reactions, and dehydrogenation, take place (Peng et al. 1998). In possible situations, advanced high stabilization temperatures (400-450 °C) are also used. In addition to using air as a stabilization medium, ozone-enriched air (Hou et al. 2008), pure oxygen medium (Bahl and Manocha 1975), ammonia (Bhat et al. 1993), sulfur dioxide (SO_2) (Błażewicz 1989), bromine and oxygen (Br_2/O_2) mixture (Peebles 2018), mixtures of hydrochloric acid vapor and oxygen (HCl/O_2) (Shindo and Nakanishi 1975) are also used for this purpose. Low-temperature pyrolysis of precursor fibers in the presence of a reactive atmosphere, such as air or oxygen, is commonly used to increase carbonization efficiency and process speed (Zhang et al. 2021; Zeng et al. 2020). The slow heating rate during the thermal stabilization phase outcomes in more carbonization yield. But is lower economical owing to long heating times (Karacan and Erzurumluoglu 2015). Impregnation of precursor fibers with appropriate flame retardant chemicals significantly improves carbon yield and carbonization rate (Peng et al. 1998).

The primary objective of this work was to evaluate structural transformations in PA-BA impregnated industrial hemp fibers during thermo-oxidative stabilization at temperatures ranging from 150°C to 250°C, prior to carbonization and activation. Experimental investigations focused on understanding the PA-BA mixture's influence during 30-minute stabilization treatments. An integrated analytical approach combining physical measurements (thickness, linear density, and tensile properties) with advanced characterization methods (DSC, TGA, FT-IR, XRD, SEM) was employed to systematically monitor structural evolution.

Experimental

Materials

FILOFIBRA AS., a Turkish supplier, provided the semi-wet drawn hemp fibers of textile-grade quality for commercial use. In our experiments, we worked with fibers having a consistent thickness of 19.1±0.2 µm and a linear density measurement of 66.6 tex. The ethanol (95%) was supplied by TEKKİM Chemical Industry, Turkey. The phosphoric acid (85%) and boric acid (99.5%) were supplied by AFG Bioscience, USA, and ZAG Kimya, Turkey, respectively.

Samples Preparation

The hemp yarn samples underwent a thorough cleaning process to eliminate dirt and dust impurities. This involved soaking in a 5% (v/v) ethanol-water solution at 60°C for one hour, followed by a 30-minute rinse under running water. For chemical impregnation, fibers were treated in a PA-BA mixture solution (pH 1.57 at process temperature) for 30 minutes at room temperature. Post-immersion, samples were blot-dried with cloth and oven-dried at 50°C for 24 hours, resulting in an approximate 8.1% PA-BA loading. Thermal stabilization was performed at five different temperatures (150-250°C in 25°C increments) for 30 minutes each, employing a controlled heating rate of 1°C/min (as illustrated in Fig. 2). To maintain molecular orientation and minimize physical shrinkage during heat treatment, samples were secured in stainless steel frames.

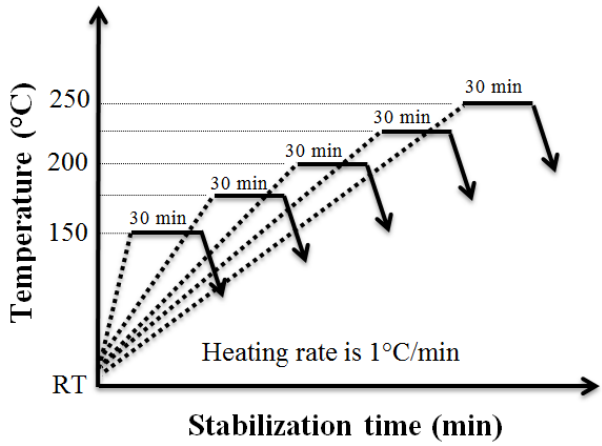

Fig. 2 The heat treatment procedure applied in the stabilization of fibers

Data Collection

Fiber Thickness Measurement and Burning Behavior Test

The flammability characteristics of oxidized hemp fibers were assessed through a basic flame test. Samples were classified as either combustible or non-combustible based on their ability to sustain burning when exposed to direct flame. For dimensional analysis, thickness variations between oxidized and untreated fibers were examined using a calibrated SOIF B_2O_3 light microscope (USA). Measurements involved five distinct fibers, with twenty measurement points taken along each fiber's length. Yarn fineness evaluation employed the linear density method, where tex values represent the weight in grams per 1000 meters of yarn. Oxidation efficiency (oxidat. effic.) was calculated as the ratio of stabilized sample linear density to raw sample linear density at each stabilization temperature.

X-ray Diffraction (XRD) Analysis

XRD analysis was conducted using a Bruker® AXS-D8-Advance diffractometer equipped with nickel-filtered Cu Kα radiation (λ = 0.154057 nm) operating at 40 kV and 40 mA. Scattering data were collected in the equatorial plane across a 2θ range of 5-45°, with an angular resolution of 0.1° per step. The diffraction profiles of both untreated and stabilized hemp fibers were analyzed using the curve deconvolution method developed by Hindeleh et al. (1983). Four distinct crystalline reflections - $(1\bar{1}0)$, (110), (020), and (004) - were identified in the equatorial diffraction patterns. Crystallinity percentages were determined through quantitative analysis of the resolved peaks using Equation (1), where the integrated intensity of crystalline regions is normalized against the total scattering intensity above the amorphous background.

$$X_C = \frac{\int_0^\infty I_{cr}\,(2\theta)d(2\theta)}{\int_0^\infty I_{tot}\,(2\theta)d(2\theta)} \tag{1}$$

Differential Scanning Calorimetry (DSC)

DSC tests were performed using a Shimadzu DSC instrument. All powdered samples were prepared with a consistent mass range of 5-6 mg for analysis. The thermal program employed a constant heating rate of 10°C/min, terminating at a maximum temperature of 500°C. Throughout the experiments, a nitrogen purge flow of 50 mL/min was maintained. DSC results were quantitatively evaluated using Equation (2), which incorporates both the enthalpy of untreated hemp fibers (ΔHo) and that of stabilized samples (ΔH) to determine the conversion index.

$$\text{DSC} - \text{conversion index } (\%) = \frac{\Delta H_0 - \Delta H}{\Delta H_0} \text{ x } 100\% \quad (2)$$

Thermogravimetric Analysis (TGA)

The thermal degradation attitude of both raw and thermally stabilized samples was investigated using a SII 7200 TG/DTA analyzer. Powdered specimens weighing 5-6 mg were prepared for each test run. Thermal profiling consisted of a linear temperature ramp at 10°C/min under a constant nitrogen atmosphere (200 mL/min flow rate), with a final isothermal hold at 700°C. TGA data interpretation focused on two key parameters: (1) progressive mass loss patterns and (2) final carbon yield percentages as functions of temperature elevation.

Fourier Transform Infrared (FT-IR) Analysis

Infrared spectral analysis was conducted in transmittance mode employing Shimadzu® Spectrum series spectrometers. Spectral acquisition covered the mid-infrared region (500-3600 cm^{-1}) with a consistent resolution of 4 cm^{-1}. The spectroscopic data revealed temperature-dependent variations in functional group characteristics throughout the thermal stabilization process of hemp fibers.

Scanning Electron Microscopy (SEM) Analysis

The sample preparation for SEM analysis involved two sequential steps: (1) deposition of a gold coating using a Cressington 108auto sputter coater, followed by (2) surface imaging with a ZEISS EVO/LS10 scanning electron microscope. For untreated hemp fiber and stabilized at 250ºC fiber, surface, and cross-sectional shape images were studied at x10000 magnification ratios. Thus, information about the surface structure and morphology of the samples was obtained.

Tensile Testing

The tensile properties of untreated and stabilized hemp fibers were attained using a Shimadzu® tensile tester. Tensile testing of the fibers was performed using a gauge length of 25 mm and a speed of 3 mm/minute. To prevent slippage of the yarns during the test, a fixed adhesive tape mounting board was employed. Owing to the fragile nature of the stabilized fibers, it was hard to divide the individual filaments, so the tensile test was performed as a yarn. The reported values are averages of at least 15 tests. The graph of each fiber break test is shared collectively.

Results and Discussion

Physical Properties

Thermal stabilization of hemp fibers impregnated with 8.1 wt% PA-BA mixture was conducted at temperatures ranging from 150°C to 250°C (30 minutes at each temperature) under atmospheric conditions. Progressive color transformations were observed with increasing treatment temperatures: golden yellow (150°C), light brown (175°C), dark brown (200°C), and finally black at both 225°C and 250°C (see Table 1 and Fig. 3). These visual changes serve as a qualitative indicator of thermal stabilization progress, corresponding to the development of cross-linked and aromatized molecular structures through oxidative dehydration reactions.

Fig. 3 Color change of untreated and PA-BA-pretreated then stabilized hemp fibers

Table 1 The physical properties of untreated and stabilized hemp fibers

Stabilization temperature (°C)	Color	Burning	Fiber thickness (micron)	Fiber thickness loss (%)	Linear density (Tex)	Linear density loss (%)	Oxidat. efficient (%)
Untreated	White	Burned	19.1	0	66.6	0	100
150	Gold Yellow	Burned	17.8	7	60.1	10	90
175	Light Brown	Burned	16.7	13	57.4	14	86
200	Dark Brown	Burned	14.2	25	51.8	22	78
225	Black	Burned	11.9	38	46.2	31	69
250	Black	Not- burned	10.1	47	42.8	36	64

Table 1 presents the temperature-dependent variations in fiber thickness during thermal stabilization. Analysis reveals a consistent reduction in hemp fiber dimensions correlating with increasing oxidation temperatures. The most significant dimensional change occurred at 250°C, showing approximately 57% thickness reduction relative to untreated fibers. These abrupt decreases in both thickness and linear density parameters correspond to mass loss during cellulose dehydration in the stabilization process (Karacan and Soy, 2013b). Concurrently, oxidation efficiency demonstrated an inverse relationship with temperature, declining progressively from 100% to 64% as stabilization temperatures increased to 250°C. A simple lighter testing was applied to evaluate the burning behavior of oxidized hemp fibers. The lighter test results are listed in Table 1 and it was seen that the hemp fiber impregnated with PA-BA and then stabilized at 250°C passed this test successfully. This showed that the hemp fiber stabilized at 250°C had sufficient thermal stability and was ready for the subsequent high temperatures.

X-ray Diffraction (XRD)

As natural cellulosic materials, untreated hemp fibers possess a cellulose II crystalline structure. These fibers exhibit 15-20% higher crystallinity than conventional lignocellulosic fibers (Le Troedec et al., 2008). Figure 4 presents the equatorial XRD patterns of hemp fibers at various stabilization temperatures, revealing four prominent crystalline peaks. Through curve-fitting analysis, we identified these reflections at $2\theta = 15.3°$ ($1\bar{1}0$), 16.7° (110), 22.5° (020), and 34.6° (004), characteristic of cellulose II (Sengupta et al., 2024; Barbash et al., 2022). The minimum intensity (I_{am}) occurred at 18.6° between the 002 and 110 peaks. Quantitative analysis using Equation (1) determined an initial crystallinity of 55.7%, which progressively decreased with rising stabilization temperatures.

The data demonstrate a clear decrystallization trend: at 250°C, the crystalline phase diminished to 11% (from 55.7%), while the amorphous fraction increased to 89% (from 44.3%). This thermal amorphization, evidenced by XRD peak reduction in Fig. 4, results from PA-BA-induced stabilization promoting cross-linked aromatic structures at the expense of crystalline domains. (Karacan and Gül 2014).

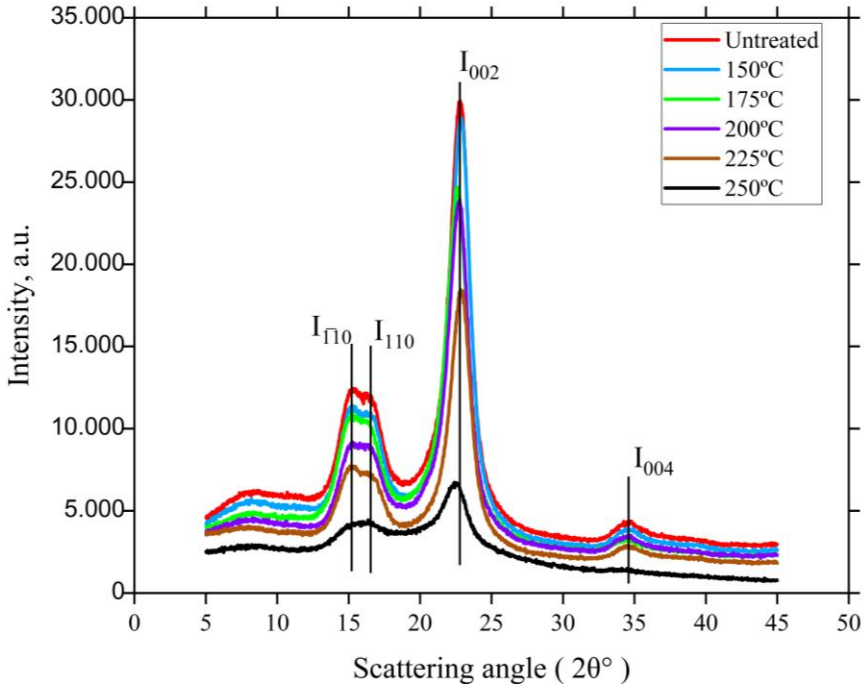

Fig. 4 Equatorial X-ray diffraction traces of samples obtained at different stabilization temperatures

Differential Scanning Calorimetry (DSC)

DSC serves as a primary analytical method for investigating thermal characteristics in polymeric systems. The DSC thermograms acquired in this study, presented in Figure 5, offer crucial insights into molecular-level structural modifications of both untreated and stabilized hemp fibers.

For untreated fibers (Fig. 5a), the thermogram displays an initial endothermic peak at ~78°C, corresponding to surface moisture evaporation. A more pronounced endothermic transition appears between 287-390°C, with peak maximum at 344°C, indicative of levoglucosan formation through cellulose depolymerization (Karacan and Gül, 2014). Following PA-BA impregnation and thermal stabilization (150-250°C for 30 minutes under oxidative conditions), significant alterations in thermal behavior were observed. Figures 5b-g demonstrate how the DSC profiles evolve with increasing stabilization temperature, reflecting the progressive structural transformations in the fiber matrix.

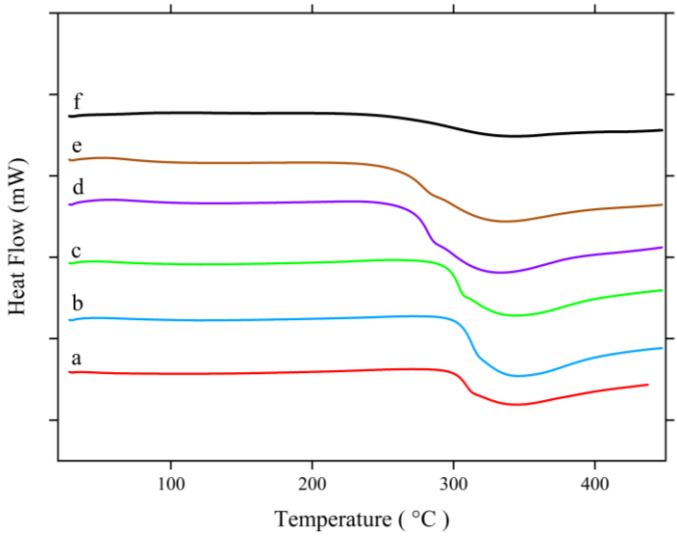

Fig. 5 DSC thermograms of samples obtained at different stabilization temperatures (a) untreated hemp fiber; (b) stabilized at 150°C; (c) stabilized at 175°C; (d) stabilized at 200°C; (e) stabilized at 225°C; (f) stabilized at 250°C

The DSC thermograms of samples stabilized at 150-175°C reveal a 10°C downward shift in cellulose depolymerization endotherms (peaking at 334°C) compared to untreated fibers. This temperature reduction stems from the flame-retardant action of the PA-BA mixture, which catalyzes cellulose decomposition through two mechanisms: (1) chemical interaction between cyclic boron phosphate ions (PBO_4) and cellulose hydroxyl groups, and (2) promoted dehydration reactions. As evidenced in Karacan and Soy's work (2013b), this catalytic effect correlates with decreasing crystallinity ratios at higher oxidation temperatures following PA-BA treatment.

The observed reduction in endothermic area at 344°C primarily stems from dehydration reactions catalyzed by boron phosphate compounds interacting with the CH_2OH hydroxyl groups in hemp cellulose. These reactions facilitate water molecule elimination between adjacent hydroxyl groups while concurrently generating C=C/C=O bonds (to be discussed subsequently). Crucially, this dehydration process minimizes volatile byproduct formation, thereby preserving the cellulose matrix - with mass loss occurring predominantly through water elimination (Dumanlı and Windle, 2012).

As stabilization temperatures exceed 225°C (Table 2), the degradation endotherm area diminishes significantly. This phenomenon correlates directly with enhanced carbonization efficiency at elevated oxidation temperatures following PA-BA treatment. The near-complete disappearance of cellulose II

degradation endotherms at 250°C (Fig. 5g) confirms the development of thermally stable, cross-linked aromatic networks. Quantitative analysis using Equation (2) reveals progressive increases in DSC conversion indices with treatment temperature, culminating in a 77% value for 250°C-stabilized samples (Table 2). This trend substantiates the temperature-dependent advancement of stabilization reactions.

Table 2 Analysis of the data acquired from the DSC

Stabilization temperature (°C)	Heating rate (°C/min)	Exotherm onset (°C)	Exotherm peak (°C)	Exothermic heat (ΔH) (J/g)	DSC conversion index (%)
Untreated	10	287	344	108	0
150	10	284	334	49	53
175	10	275	332	47	57
200	10	245	327	38	69
225	10	232	322	27	72
250	10	229	318	16	77

Thermogravimetric Analysis (TGA)

With the TGA, the thermal stability and decomposition properties of untreated and PA-BA-impregnated hemp fibers were analyzed. TGA curves showing sample weight losses at different oxidation temperatures (between 150 and 250°C) depending on temperature are shared in Fig. 6. When the obtained graphs were analyzed, it was seen that the weight falls occurring around 55-90 °C represented the evaporation called surface water. The TGA thermogram of untreated hemp showed significant weight loss at temperatures between 300 and 500°C. The decomposition process of untreated hemp fibers begun at 300°C and go on until approximately 500 °C. In this test carried out in a nitrogen environment, it is seen that the significant decomposition reaction takes place in these temperature ranges, and the highest weight loss occurs at 355°C. In the absence of any treatment, hemp fiber exhibits a carbon yield of approximately 11% at a temperature of 700°C. In contrast, thermograms of PA-BA-impregnated and stabilized hemp fibers demonstrated a reduction in weight loss with increasing oxidation temperature. This revealed the increased carbon yield due to interchain cross-linking and aromatization reactions of cellulose-hemicellulose and lignin in the structure of hemp.

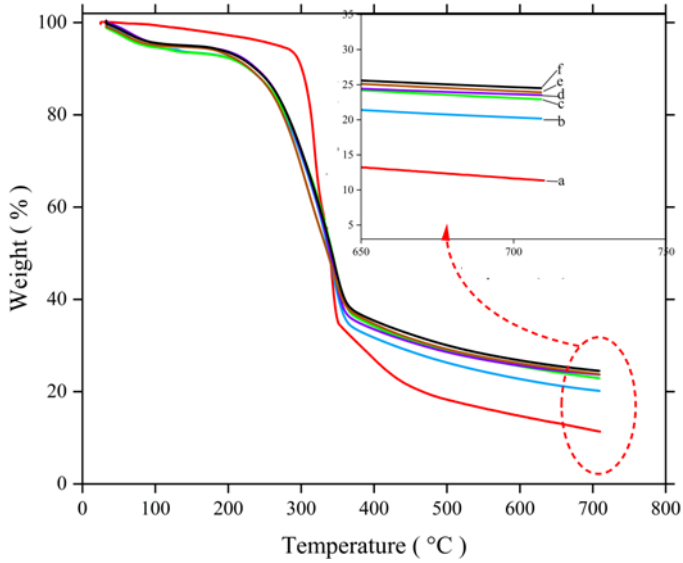

Fig. 6 TGA thermograms of samples obtained at different stabilization temperatures (a) untreated hemp fiber; (b) stabilized at 150°C; (c) stabilized at 175°C; (d) stabilized at 200°C; (e) stabilized at 225°C; (f) stabilized at 250°C

Figure 7 compares the carbon yields (%) of untreated and stabilized hemp fibers at 350 and 700°C for the determined oxidation temperatures. These results once again revealed that the carbon yield continuously increases as a function of increasing stabilization temperature. The obtained data revealed results consistent with similar studies previously conducted in the literature (Hariri et al. 2024). The carbon yields at 350°C were found to exhibit a range of 41% to 45% across oxidation temperatures between 150 and 250°C. With regard to the carbon yield at 700 °C, the highest value was observed to be 25% for PA–BA impregnated hemp fiber oxidized at 250°C. It was revealed by TGA tests that PA-BA-impregnated and stabilized hemp fibers showed higher thermal stability owing to cross-linking. This demonstrated higher thermal stability can be pointed to the more efficient cross-linking and aromatization reactions catalyzed with PA-BA. It can be said that the hydroxyl groups in the cellulose structure and impregnation chemicals have a strong interaction. This shows that it leads to both intramolecular and intermolecular cross-linking.

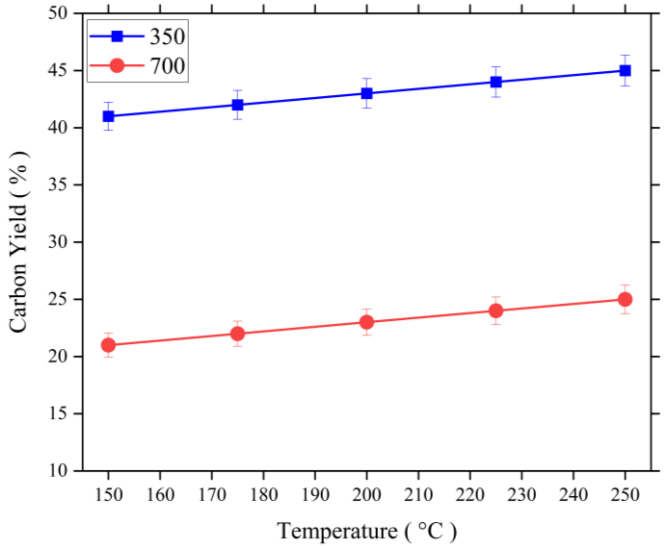

Fig. 7 Change of carbon yields of stabilized hemp fibers 350°C (■) and 700°C (●)

Fourier-transform Infrared Spectroscopy (FT-IR)

FT-IR served as a primary analytical tool for monitoring molecular transformations during thermal stabilization. This technique proved particularly valuable for characterizing hydrogen bonding patterns within the cellulose matrix and identifying structural modifications in cellulose, hemicellulose, and lignin components. The infrared spectra (3600-500 cm^{-1}) displayed in Figure 8 compare untreated and PA-BA treated hemp fibers across various stabilization temperatures. Enhanced borate/phosphate (BO_4/PO_4) formation at lower temperatures, facilitating cross-linking and dehydration Characteristic hydroxyl stretching (3600-3100 cm^{-1}) from intra- and intermolecular hydrogen bonds (Oh et al., 2005). Methyl group vibrations (2850-3000 cm^{-1}). Cellulose II fingerprint regions (1425, 1377, 1332, 1317, 1247, 1227, 1110, and 910 cm^{-1}) confirming crystalline structure (Sawpan et al., 2011). The spectral data demonstrate how chemical treatment modifies the fiber's molecular architecture during thermal processing.

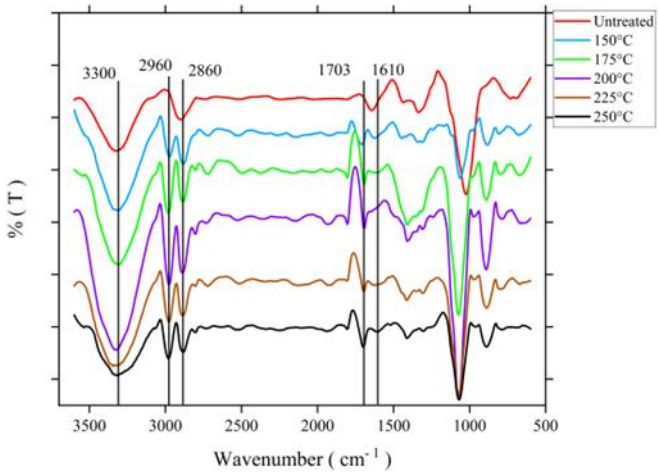

Fig. 8 FT-IR bands of stabilized hemp fibers and untreated

As stabilization temperatures increased, the intensity of methyl (-CH) group vibrations (3000-2780 cm^{-1}) progressively diminished without complete disappearance in FT-IR spectra. This attenuation indicates disruption of intermolecular hydrogen bonding networks within the cellulose matrix. According to Oh et al. (2005), the observed growth in amorphous content directly correlates with both declining crystallinity and breaking of these hydrogen bonds during thermal treatment. FT-IR analysis revealed significant spectral changes with increasing stabilization temperatures. The carbonyl (C=O) stretching vibration at 1703 cm^{-1} showed progressive intensity enhancement, accompanied by the formation of a new absorption band. Notably, a distinct peak emerged at 1610 cm^{-1}, corresponding to C=C stretching vibrations. This aromatic signature became particularly prominent in the 250°C-stabilized sample, confirming the development of conjugated aromatic systems within the oxidized cellulose matrix. The presence of boron phosphate groups facilitated two key processes: Enhanced crosslinking and dehydration at reduced temperatures and selective blocking of primary hydroxyl groups, thereby inhibiting volatile byproduct formation (Karacan and Gül 2014).

Scanning Electron Microscopy (SEM)

SEM was employed to examine morphological differences between untreated hemp fibers and those stabilized at 250°C following PA-BA impregnation. Figure 9 presents comparative micrographs of (a) untreated fibers and (b) chemically treated/stabilized specimens. Comparative cross-sectional views (highlighted in red frames) demonstrate significant surface differences. The untreated fiber sample displays pronounced longitudinal striations originating from the mechanical processing during fiber isolation. The cross-sectional morphology

deviates from a perfect cylindrical form, exhibiting instead a fractured cylindrical appearance. Comparative analysis of the micrographs reveals the disappearance of the fibrous bundle structure present in untreated samples following 250°C stabilization. These morphological alterations demonstrate significant physical transformation during thermal processing, evidenced by: (1) loss of structural integrity and (2) measurable changes in cross-sectional geometry. Microscopic examination reveals minimal residual chemical deposits on fiber surfaces, even at negligible levels. The observed surface homogeneity in 250°C-stabilized fibers stems from two key factors: (1) intrinsic material properties of the hemp precursor, and (2) controlled thermal stabilization following chemical treatment. This optimized processing yields preserved surface morphology while promoting structural uniformity - a critical prerequisite for subsequent carbonization stages.

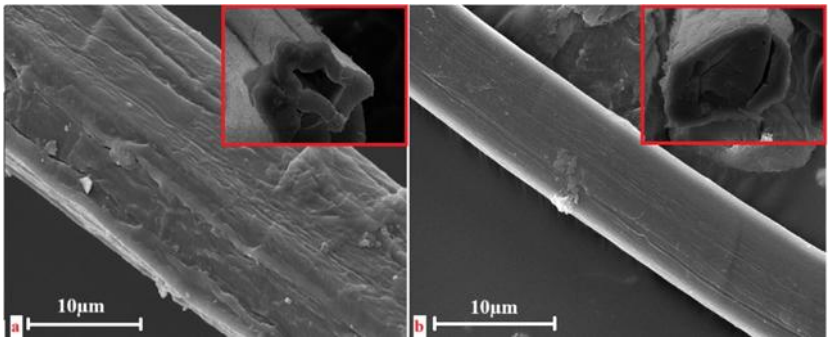

Fig. 9 SEM images of (a) untreated hemp fiber and (b) stabilized fiber at 250°C

Tensile Properties

The mechanical properties are expressed as follows: tensile force (N), elongation at break (%), and elastic modulus (N/tex). With the increase in the oxidative stabilization temperature, the tensile force in the samples decreases up to 225°C, while a partial increase is observed in the 250°C sample (Table 3, Fig. 10). With the increase in the stabilization temperature, the cellulose structure gradually deteriorates due to the loss of crystalline structure and the increase in amorphous structure formation in the samples. The increase in the stabilization temperature from 150°C to 225°C causes the hydrogen bonds (or bridges) between the polymer chains formed by the cellulose rings to break. The hydrogen bridges that disappear between the cellulose chains cause a loss of strength. The increase in strength seen at 250°C is due to the formation of cyclization reactions and the formation of cross-links between the chains. The stabilization stage before carbonization was partially completed with the hemp fiber obtained at

250°C. It is thought that this sample is ready for the carbonization stage and has gained resistance to high temperatures.

Table 3 The mechanical properties of untreated and stabilized hemp fibers

Stabilization temperature (°C)	Tensile force (N)	Extension at break (%)	Elastic modulus (N/Tex)
Untreated	20,86	5,97	0,313
150	2,75	0,28	0,046
175	2,49	0,24	0,043
200	1,62	0,25	0,031
225	1,26	0,26	0,027
250	1,39	0,39	0,032

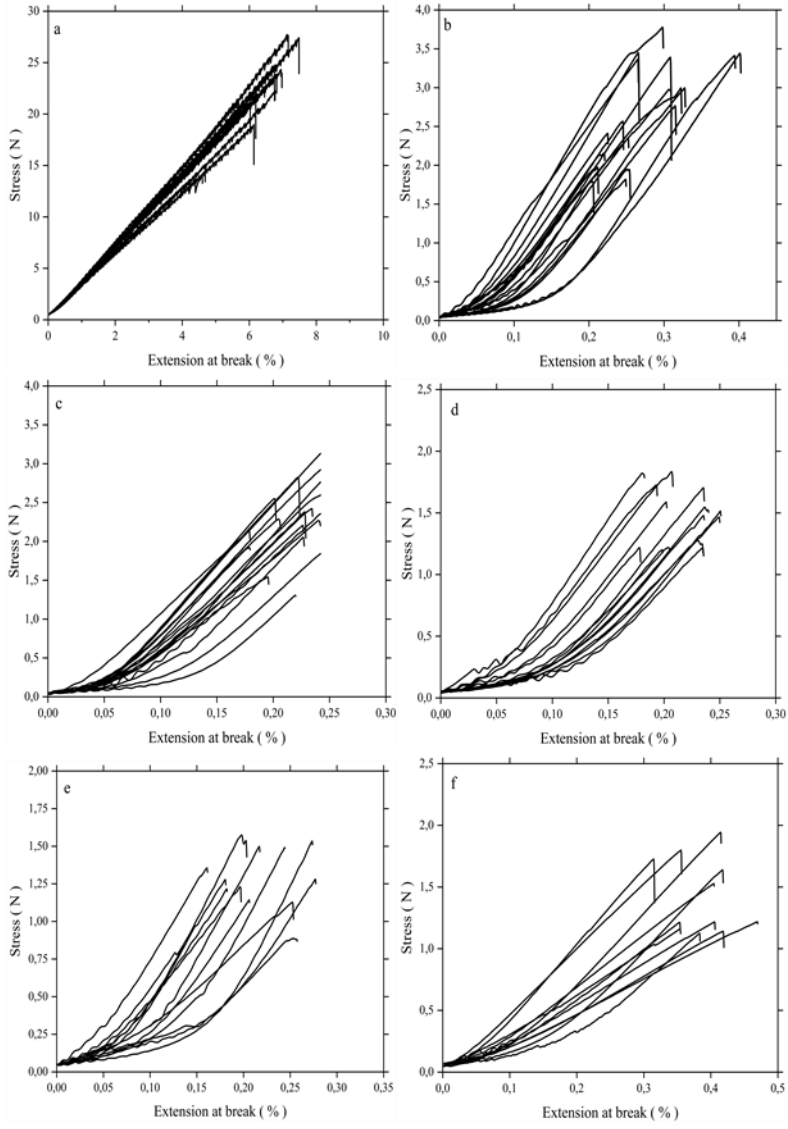

Fig. 10 Stress-strain curves at different stabilization temperatures (a) untreated hemp fiber; (b) stabilized at 150°C; (c) stabilized at 175°C; (d) stabilized at 200°C; (e) stabilized at 225°C; (f) stabilized at 250°C

Conclusions

After wet treatment with an aqueous solution of 4% PA and 4% BA, industrial hemp fibers were subjected to thermal stabilization processes at 150, 175, 200, 225, and 250°C for holding times of 30 minutes each. The obtained outputs revealed that PA-BA mixture impregnation positively affected the oxidative stability of hemp fibers. Thermal stabilization at 250°C led to the breakdown of cellulose II crystallinity, caused by amorphous transformations resulting from the loss of both intra- and intermolecular hydrogen bonding. The outcomes acquire from fiber thickness, linear density, carbon yield %, X-ray diffraction, FT-IR, and tensile test measurements showed that the stabilization temperature was effective in the stabilization of hemp fibers. The samples obtained from hemp fibers stabilized in an oxidative environment showed physical and chemical changes with increasing stabilization temperature. The samples exhibited a decrease in fiber thickness and linear density worths, accompanied by a decline in tensile force, and tensile modulus values. This was observed following the elimination of volatile substances, including H_2O, CO, and CO_2. The results obtained from linear density calculations showed a decrease of 36% at the stabilization temperature of 250ºC, indicating about 64% oxidation efficiency. X-ray diffraction tests exhibited that the crystalline form of cellulose II structure became increasingly amorphous with the increase in stabilization temperature. Infrared spectroscopy exhibited the loss of OH, CH, C=O, CH_2, C–O, and C–O–C groups owing to the removal of hydrogen and oxygen atoms due to completely completed dehydration and dehydrogenation reactions. Although there was a decrease in mechanical properties with the increase of the stabilization temperature from 150ºC to 225ºC, a partial increase was observed for 250ºC. These results show that mechanical properties are reduced as a result of the destruction of hydrogen bridges between the cellulose rings during stabilization and the transformation of the crystal structure into an amorphous structure. The consequences acquired from X-ray diffraction and FT-IR spectroscopy analyses exhibited that cellulose disappear most of its crystalline structure owing to the forming of an amorphous structure throughout the stabilization reactions. Hemp fiber stabilized at 250ºC acquired a high-temperature resistant structure and was ready for the next stage of carbonization.

Acknowledgements

This study was supported by Scientific and Technological Research Council of Türkiye (TUBITAK) under the Grant Number 223M375. The authors thank to TUBITAK for their supports.

References

Bahl, O.P., Manocha, L.M., (1975). Effect of preoxidation conditions on mechanical properties of carbon fibres. *Carbon*, 13:(4) 297-300. https://doi.org/10.1016/0008-6223(75)90032-9

Baker, D.A., Rials, T.G., (2013). Recent advances in low-cost carbon fiber manufacture from lignin. *J Appl Polym Sci* 130:713– 728. https://doi.org/10.1002/app.39273

Barbash, V.A., Yashchenko, O.V., Yakymenko, O.S., Zakharko, R.M., Myshak, V.D., (2022). Preparation of hemp nanocellulose and its use to improve the properties of paper for food packaging. *Cellulose* 29:8305–8317. https://doi.org/10.1007/s10570-022-04773-6

Bengtsson, A., Bengtsson, J., Jedvert, K., Kakkonen, M., Tanhuanpää, O., Brännvall E, Sedin, M., (2022). Continuous Stabilization and Carbonization of a Lignin–Cellulose Precursor to Carbon Fiber. *ACS Omega*, 7(19):16793-16802. https://doi.org/10.1021/acsomega.2c01806

Bhat, G.S,, Peebles, Jr L.H., Abhiraman, A.S., Cook, F.L., (1993). Rapid stabilization of acrylic fibers using ammonia: effect on structure and morphology. *J App Poly Sci* 49:(12) 2207-2219. https://doi.org/10.1002/app.1993.070491217

Bengtsson, A., Bengtsson, J., Sedin, M., Sjöholm, E,, (2019). Carbon fibers from lignin-cellulose precursors: effect of stabilization conditions. *ACS Sustainable Chemistry & Engineering* 7 (9):8440–48. https://doi:10.1021/acssuschemeng.9b00108.

Błażewicz, S., (1989). Carbon fibres from a SO_2 treated PAN precursor. *Carbon* 27:(6) 777-783. https://doi.org/10.1016/0008-6223(89)90027-4

Bortner, M.J. (2003). Melt Processing of Metastable Acrylic Copolymer Carbon Precursor Ph D Thesis Dissertation Submitted to the Faculty of Virginia Polytechnic Institute and State University,

Borsa, J., László, K., Boguslavsky, L., Takács, E., Rácz, I., Tóth, T., Szabó, D. (2016). Effect of mild alkali/ultrasound treatment on flax and hemp fibres: the different responses of the two substrates. *Cellulose* 23:2117–2128. https://doi.org/10.1007/s10570-016-0909-y

Byrne, N., De Silva, R., Ma, Y. et al (2018). Enhanced stabilization of cellulose-lignin hybrid filaments for carbon fiber production. *Cellulose* 25:723–733. https://doi.org/10.1007/s10570-017-1579-0

Chand, S. (2000). Review carbon fibers for composites. *J Mater Sci* 35:1303-1313. https://doi.org/10.1023/A:1004780301489.

Dumanlı, A.G., Windle, A.H. (2012). Carbon fibres from cellulosic precursors: a review. *J Mater Sci* 47:4236–4250. https://doi.org/10.1007/s10853-011-6081-8

Edison, TA (1880) Electric Lamp, U. S. Patent 223 898,

Fu, R., Liu, L., Huang, W., Sun, P. (2003). Studies on the structure of activated carbon fibers activated by phosphoric acid. *J Appl Polym Sci* 87:2253–2261. https://doi.org/10.1002/app.11607

Fukuzumi, H., Saito, T., Okita, Y., Isogai, A. (2010). Thermal stabilization of TEMPO-oxidized cellulose. *Polym Degrad Stab* 95:1502–1508 https://doi.org/10.1016/j.polymdegradstab.2010.06.015

Gregorová, A., Košíková, B., Moravčík, R. (2006). Stabilization effect of lignin in natural rubber. *Poly Degradation and Stability* 91:229–233. https://doi.org/10.1016/j.polymdegradstab.2005.05.009

Hariri, H., Tunçel, K.Ş., Karacan, I. (2024). Structure and Properties of Thermally Stabilized and Ecologically Friendly Organic Cotton Fibers as a New Activated Carbon Fiber Precursor. *Fibers and Polymers* 25:2925–2933. https://doi.org/10.1007/s12221-024-00648-8

Hindeleh, A.M., Johnson, D.J., Montague, P.E. (1983). Fibre Diffraction Methods', ACS Symp. French AD and Gardner KH edn. American Chemical Society, Washington DC, pp 149-181

Hou, Y., Sun, T., Wang, H., Wu, D. (2008). Influence of ozone on chemical reactions during the stabilization of polyacrylonitrile as a carbon fiber precursor. *J App Poly Sci* 108:(6) 3990-3996. https://doi.org/10.1002/app.27939

Huang, X. (2009). Fabrication and properties of carbon fibers. *Materials* 2(4):2369-2403. https://doi.org/10.3390/ma2042369.

Il, K.M., Park, M.S., Lee, Y.S. (2016). Cellulose-based carbon fibers prepared using electron beam stabilization. *Carbon Lett* 18:56–61. https://doi.org/10.5714/CL.2016.18.056

Kabir, M.M., Islam, M.M., Wang H (2013). Mechanical and thermal properties of jute fibre reinforced composites. *J Multifunctional Composites* 1(1):71–77. https://doi:10.12783/.2168-4286/1.1/Islam.

Karacan, I., Erzurumluoğlu, L. (2015). Formation of non-graphitizing carbon fibers prepared from poly (p-phenylene terephthalamide) precursor fibers. Fibers and Polymers 16(5):961-974. https://doi.org/10.1007/s12221-015-0961-5

Karacan, I., Gül, A. (2014). Carbonization behavior of oxidized viscose rayon fibers in the presence of boric acid–phosphoric acid impregnation. J Mater Sci 49:7462-7475. https://doi.org/10.1007/s10853-014-8451-5

Karacan, I, Soy, T., (2013a). Structure and properties of oxidatively stabilized viscose rayon fibers impregnated with boric acid and phosphoric acid prior to carbonization and activation steps. *J Mater Sci* 48:2009-2021. https://doi.org/10.1007/s10853-012-6970-5

Karacan, I., Soy, T., (2013b). Investigation of structural transformations taking place during oxidative stabilization of viscose rayon precursor fibers prior to carbonization and activation. *J Mol Str* 1041:29-38. https://doi.org/10.1016/j.molstruc.2013.02.040

Le Troedec, M., Sedan, D., Peyratout, C., Bonnet, J.P., Smith, A., Guinebretiere, R., Krausz, P. (2008). Influence of various chemical treatments on the composition and structure of hemp fibres. Composites Part A: *Applied Science and Manufacturing* 39(3):514-522. https://doi.org/10.1016/j.compositesa.2007.12.001

Li, K., Li, Y., Hu, H. (2011). Adsorption characteristics of lead on cotton-stalk-derived activated carbon fiber by steam activation. *Desalination and Water Treatment* 30:1–9. https://doi.org/10.5004/dwt.2011.1130

Liu, H., Zhang, S., Yang, J., Ji, M., Yu, J., Wang, M., Chai, X., Yang, B., Zhu, C. et al (2019). Preparation, Stabilization and Carbonization of a Novel Polyacrylonitrile-Based Carbon Fiber Precursor. *Polymers* 11(7):1150. https://doi.org/10.3390/polym11071150

Lu, Y., Lu, Y.C., Hu, H.Q., Xie, F.J., Wei, X.Y. et al (2017). Structural characterization of lignin and its degradation products with spectroscopic methods. J Spectroscopy 2017:(1) 8951658.

https://doi.org/10.1155/2017/8951658

Newcomb, BA (2016) Processing, structure, and properties of carbon fibers. Composites Part A 91:262– 282.

Oh, S.Y., Yoo, D.I., Shin, Y., Kim, H.C., Kim, H.Y., Chung, Y.S., Youk, J.H. (2005). Crystalline structure analysis of cellulose treated with sodium hydroxide and carbon dioxide by means of X-ray diffraction and FTIR spectroscopy. *Carbohydrate Research* 340(15): 2376-2391. https://doi.org/10.1016/j.carres.2005.08.007

Peebles, L.H., (2018). Carbon fibers: formation, structure, and properties. CRC Press,

Peng, J.C., Donnet, J.B., Wang, T.K., Rebouillat, S., (1998). Carbon fibers, ed. By Peng JC, Donnet JB, Wang TK, (CRC Press, New York) p. 161

Poovaiah, C.R., Nageswara-Rao, M., Soneji, J.R., Baxter, H.L., Stewart, Jr C.N., (2014). Altered lignin biosynthesis using biotechnology to improve lignocellulosic biofuel feedstocks. *J Plant Bio* 12:1163. https://doi.org/10.1111/pbi.12225

Rahman, M.M., Karacan, I. (2022a). Structural and thermal characterization of chemically pretreated and thermally oxidized bamboo fiber in activated carbon fiber manufacturing. *J Natural Fibers* 19(16): 15085–15099. https://doi.org/10.1080/15440478.2022.2070324

Rahman, M.M., Karacan, I. (2022b). The impact of eco-friendly chemical incorporation on the thermal oxidation process of flax fiber prior to carbonization and activation. *J Mater Sci* 57:2318–2333. https://doi.org/10.1007/s10853-021-06686-4

Rosas, J.M., Bedia, J.R., Rodríguez-Mirasol, J, Cordero, T. (2009). HEMP-derived activated carbon fibers by chemical activation with phosphoric acid. *Fuel* 88(1):19-26. https://doi.org/10.1016/j.fuel.2008.08.004

Sawpan, M.A., Pickering, K.L., Fernyhough, A. (2011). Effect of various chemical treatments on the fibre structure and tensile properties of industrial hemp fibres. Composites Part A: *App Sci Manufac* 42(8):888-895. https://doi.org/10.1016/j.compositesa.2011.03.008

Sengupta, S., Bhowmick, M., Basak, S., Samanta, K.K., Avijit, Das L.M., Shakyawar, D.B., (2024). Characterization of Indian hemp (Canabinus sativa L.) fiber and investigation of its potential in textile application. *Cellulose* https://doi.org/10.1007/s10570-024-06009-1

Shindo, A., Nakanishi, Y., Sawada, Y. (1975). Method for manufacture of heat-resistant fibers. United States Patent number US 3,886,263.

Williams, P.T., Reed, A.R. (2004). High grade activated carbon matting derived from the chemical activation and pyrolysis of natural fiber textile waste. *J Analytical and App. Pyrolysis,* 71(2):971-986. https://doi.org/10.1016/j.jaap.2003.12.007

Zeng, F., Liao, X., Pan, D., Shi, H. (2020). Adsorption of dissolved organic matter from landfill leachate using activated carbon prepared from sewage sludge and cabbage by $ZnCl_2$. Environmental *Sci Pol Res* 27:(5) 4891-4904. https://doi.org/10.1007/s11356-019-07233-0

Zhang, Y., Zhao, M., Cheng, Q., Wang, C., Li, H., Han, X., Li Z. (2021). Research progress of adsorption and removal of heavy metals by chitosan and its derivatives: A review. *Chemosphere,* 279:130927. https://doi.org/10.1016/j.chemosphere.2021.130927

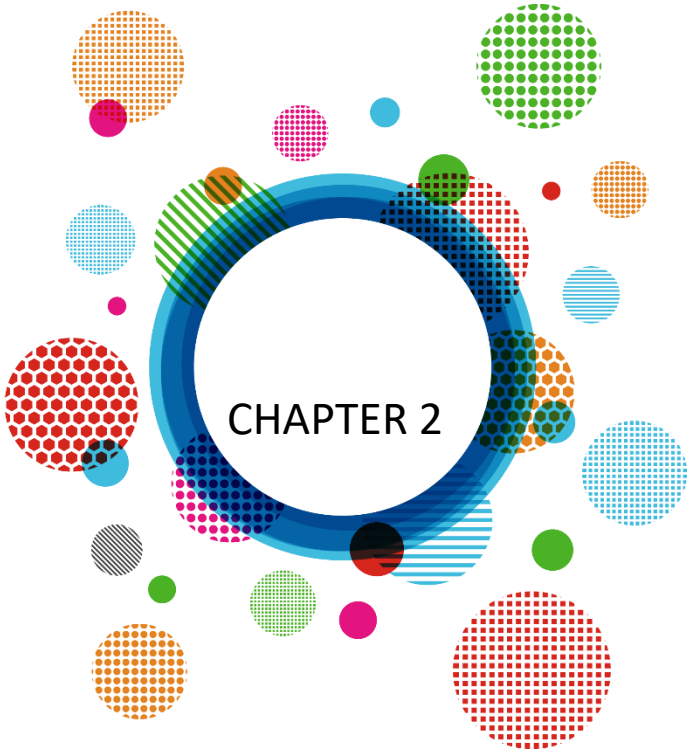

Some Structural Characterizations of Nanofibers Obtained by Electrospinning Method for the Production of Environmentally Friendly Membrane with Industrial Hemp Additives

Abdullah Gül[1] & Ismail Tiyek[2] & Ahmet Karadağ[3] & İbrahim Kılıç[4]

[1] Dr. Öğr. Üyesi, Hemp Research Institute, Yozgat Bozok University, Yozgat, 66100, Turkey, ORCID ID: 0000-0001-6990-417X, Correspondence to

[2] Doç. Dr., The Department of Textile Engineering, Kahramanmaraş Sutcu Imam University, Kahramanmaraş, 46100, Turkey, ORCID ID: 0000-0002-1643-8977

[3] Department of Chemistry, Science and Letters Faculty, Bursa Uludağ University, Bursa 16059, Türkiye ORCID ID: 0000-0003-4676-683X

[4] Dr. Öğr. Üyesi Department of Material and Energy, Hemp Research Institute, Yozgat Bozok University, Yozgat, Türkiye, ORCID ID: 0000-0003-0567-5923

Introduction

The method, more commonly known as electrospinning, is also referred to as electrospinning or electro-production. Electrospinning is the most effective and convenient method for nanofiber production. In its most general definition, electrospinning is the decomposition of a polymeric material in molten or solution form into nano-diameter fibers under the influence of an electric field, subjected to a high voltage. Electrospinning is an interdisciplinary method encompassing polymer chemistry, fluid dynamics, electrical physics, fundamental physics, textile, and mechanical engineering (Yıldırım, 2016).

Electrospinning essentially involves spraying a polymer solution or melt with an electrical charge from a syringe or capillary tip. The resulting polymer jet is generated by connecting the electrodes of an electrical power source and drawing it from the needle tip to the collector plate, depending on the electric field strength. The evaporation of the solution causes fibers to form and accumulate on the collector plate. It is recommended to use solutions with relatively high polymer concentrations to obtain filaments (continuous fibers). The diameter of the resulting fibers varies between micrometers and nanometers. Fiber diameters can be adjusted by changing the processing standards (Subbiah et al., 2005).

Electrospinning is a highly economical and efficient method for producing nanofibers from many different polymer derivatives (Tian et al., 2011). The structures formed by electrospun fibers create a high surface area and volume. In addition, they contain extremely small pores. Therefore, they are finding applications in many fields, including nanocatalysis, tissue engineering, protective textiles, filtration, biomedical engineering, electronics, healthcare, biotechnology, security, and environmental engineering (Suwantong et al., 2008).

Electrospinning, the most researched nanofiber production method, has faced some challenges in its industrialization due to its low production speed and high voltage requirements. Electrospinning, which operates at a voltage of approximately thousands of volts, requires extra safety precautions during production. Screw extruder systems are known to be used for industrial-level polymer melt preparation. If electrospinning is combined with extrusion using these extruder systems, the electrical voltage must be applied directly to the extruder. Due to the potential for dangerous arcing on the extruder in this case, the system requires well-designed electrical insulation (Lyons et al., 2004). Arc hazards can pose a serious danger not only to the extruder itself but also to the operator.

In the electrospinning technique (Fig. 1), a liquid polymer structure in molten or solution form is fed through a capillary tube. A high-voltage energy source applies very high voltage to the polymer solution. In this case, the surface of the

solution accumulation suspended at the tip of the needle (1) becomes electrically charged. As the applied voltage increases, the polymer droplet (2) assumes a conical shape (Taylor cone). When the voltage reaches a critical level and the repulsive forces of the charges in the droplet overcome the surface tension, a thin jet emerges from the tip of the Taylor cone (3). Based on the principle of repulsion between the same electrical charges on the jet surface, the jet lengthens and tapers, directed toward the collector. During this direction, this polymer jet initially follows a stable and then an unstable (spiral) path (5). In this case, the solvent evaporates, leaving behind polymeric fibers with nano-sized diameters. These continuous nanofibers are positioned in a regular manner on the collector plate (6) and form a nonwoven surface (Üstündağ G. 2009).

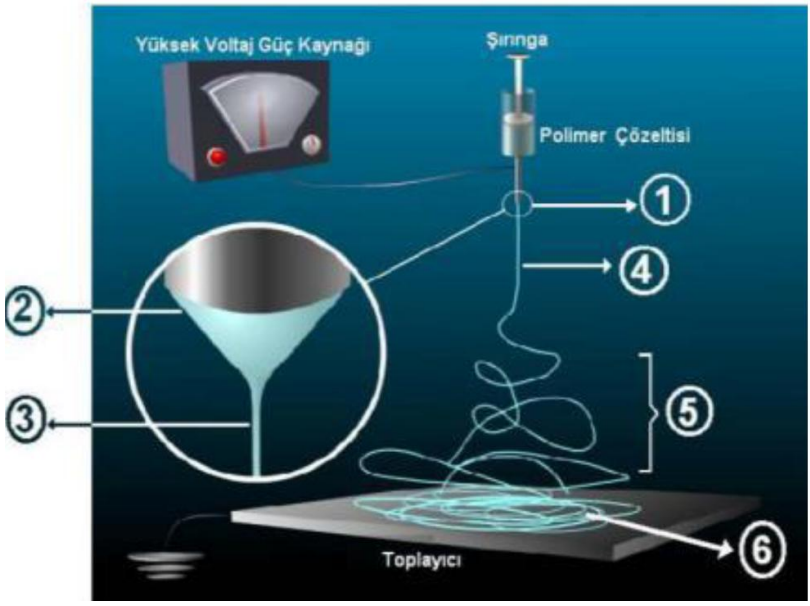

Fig.1 Electrospinning method and basic process sequence (Yıldırım, 2016).

When electrospinning polymer parameters are examined, factors such as viscosity, vapor pressure, surface tension, conductivity, molecular chain length, concentration (for solution), solubility, presence of chain-breaking agents and dielectric coefficient affect the properties of the nanofiber to be obtained (Luo et al., 2012).

Polyamide 66 (PA66), also commonly known as nylon 66, is an important polymer in the engineering plastics class. PA66 is used in a wide range of applications due to its superior properties such as high strength, stiffness, and heat

resistance. PA66 is also known for its high chemical resistance (Smith, 2019). PA66 is obtained by the polycondensation reaction of hexamethylenediamine and adipic acid (Brown, 2020). PA66 is widely used in many industries such as automotive, electrical and electronics, textiles, and consumer products (Taylor, 2020). It is particularly preferred in applications requiring components that are resistant to high temperatures and have high mechanical strength (Johnson, 2021).

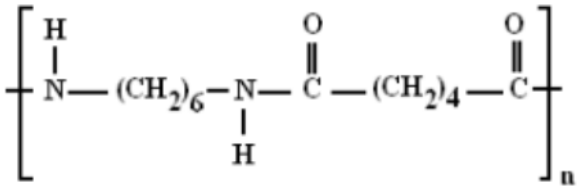

Fig. 2 Repeated chemical structure of PA66 (Rajeshbijwe, 2002).

Polyamide, a thermoplastic product, represents a class of materials with high strength, hardness, and good electrical and chemical properties, as well as being lightweight and available in many varieties. It is known to be resistant to petroleum oils, aliphatic and aromatic hydrocarbons, ketones, and ethers. Phenol, cresol, and formic acid dissolve polymers at room temperature. Alkali-based polymers are affected by strong acids and oxidizing agents. Polyamide also has good permeability to water vapor, air, and oxygen. It is resistant to bacteria and fungi (Özdemir, 2001).

Industrial hemp is a rapidly growing crop called Cannabis sativa. Hemp fibers are quite popular compared to other plants due to their high stiffness and strength, as well as their many advantages such as low cost and low density (Reddy and Yang, 2008). Hemp fibers are one of the cellulose fibers that have been used in a wide range since ancient times. Hemp has gained great importance due to its advantages such as biodegradability, rapid growth, low production costs, and ability to grow in various climatic conditions (Dhondt, 2020). Hemp fibers are composed of cellulose, hemicellulose, lignin, and pectin (Pakarinen et al., 2012). In addition to their high cellulose content, hemp fibers have various properties, including strong adsorption, breathability, antibacterial properties, good permeability, and heat transfer (Zhang et al., 2021). Hemp fiber is used in textiles, chemicals, paper, etc. It can be used in many applications, including (Westerhuis et al., 2019). In order to use hemp fibers in various sectors, it is important to know their content well.

The purpose of pretreating hemp fibers is to produce the desired fiber material from various raw materials to meet the diverse needs of future users. To achieve uniform quality, hemp fibers can be subjected to physical, chemical, physicochemical, and biological pretreatment to modify the material's chemical composition, color, and fineness.

Experimental

Materials

PA66 pellet (Formula Weight: 262.36 g/mol, Density: 1.19 g/mL), formic acid (HCOOH, >98 %), sodium hydroxide pellet (NaOH >98 %), hydrochloric acid (HCl, 37 %) and acetic acid (CH_3COOH, 100 %) were obtained from Sigma Aldrich. Hemp plant fiber (HF) plant was obtained from Yozgat Bozok University Hemp Research Institute in Turkey.

Preparation of hemp fibers

Hemp fibers were subjected to a chemical pretreatment (cleaning and bleaching) to reduce hemicellulose and lignin content. This process is generally carried out using sodium hydroxide (NaOH) to remove lignin and pectin present in hemp fibers (Zhao, 2020; Ji, 2021; Pakarinen, 2012). In this study, a 2% aqueous NaOH solution was prepared, and a mixture of hemp husk fibers was autoclaved at 121°C for 1 h. After autoclaving, the mixture was neutralized with 37% hydrochloric acid (HCl), then washed three times with distilled water, and filtered. The upper part of the mixture was removed when it reached room temperature, and the precipitated fibers were collected and dried in an oven at 50°C for 24 h. Following the chemical pretreatment, the fibers were ground into small pieces of 0.1–2 mm in a ball mill to increase solubility.

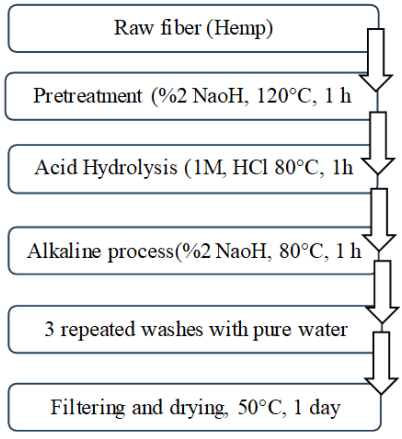

Fig. 3 Scheme of preparation of hemp fibers

Preparation of hemp-added solution

To produce nanofiber membranes, solutions containing PA66 and HF were prepared in various weight ratios, maintaining a total solid content of 10 wt%. Specifically, five different solutions were formulated with PA66/HF weight ratios of 100/0, 99/1, 96/4, 92/8, and 90/10. These samples were designated as HF-0, HF-1, HF-4, HF-8, and HF-10, respectively. The detailed mixing ratios are presented in Table 1. A solvent mixture of formic acid and acetic acid in a 3:1 ratio was used for all formulations (Fig. 4 and Table 1). Each solution was first stirred on a heated magnetic stirrer at 50 °C for 30 minutes, followed by additional mixing at room temperature for 12 hours. Finally, the solutions were treated in an ultrasonic bath for 30 minutes at room temperature to ensure complete dissolution and homogeneity.

Fig. 4 Preparation of hemp-added PA66 polymer solution

Table 1. Work plan

Order	Total Solids Ratio (%)	Solid Matter Ratio (%)	Co-solvent	Code
1	10	100 (PA66)	(3:1) FA: AA	0 H
2		99/1 (PA66/Hemp)		1 H
3		98/2 (PA66/Hemp)		2 H
4		96/4 (PA66/Hemp)		4 H
5		92/8 (PA66/Hemp)		8 H
6		90/10 PA66/Hemp)		10 H

Data Collection

Membrane Thickness Measurement

The thickness values of the membrane samples obtained by the electrospinning method were measured. Measurements were carried out in

accordance with the TS EN 29073-2 standard using an Akyol brand thickness measuring device (micrometer) with a precision of 0.001 mm at the Kahramanmaraş Sutcu Imam University USKIM Materials Technical Laboratory.

Differential Scanning Calorimetry (DSC)

DSC tests were performed using a Shimadzu DSC instrument. All samples were prepared with a consistent mass range of 5-6 mg for analysis. The thermal program employed a constant heating rate of 10°C/min, terminating at a maximum temperature of 500°C. Throughout the experiments, a nitrogen purge flow of 50 mL/min was maintained. DSC results were quantitatively evaluated using Equation (1), which incorporates both the enthalpy of untreated hemp fibers (ΔH_o) and that of stabilized samples (ΔH) to determine the conversion index.

$$\text{DSC} - \text{conversion index}\ (\%) = \frac{\Delta H_0 - \Delta H}{\Delta H_0}\ \text{x}\ 100\% \qquad (1)$$

Thermogravimetric Analysis (TGA)

In thermogravimetric analysis curves, factors that cause mass loss include evaporation of volatile components, drying, gas absorption or vaporization, thermal decomposition in environments containing inert gas, oxidation of the material, heterogeneous chemical reactions, and changes in the magnetic properties of some materials with temperature. Thermogravimetric analysis (TGA) was performed on the Exstar TG/DTA 6300 device located at the Kahramanmaraş Sutcu Imam University USKIM center, at temperatures ranging from room temperature to 650 °C and a nitrogen output rate of 100 mL/min. For membranes with nanofiber surfaces, analysis was performed at a temperature increase rate of 10 °C/min.

Fourier Transform Infrared (FT-IR) Analysis

Fourier transform infrared spectroscopy (FTIR) analysis was used to determine the functional groups of the membrane samples. The wavelength range of 400-4000 cm^{-1} was studied using the Perkin Elmer Spectrum 400 instrument, located at the Kahramanmaraş Sütçü İmam University ÜSKİM Center. Samples with nanofiber surfaces were examined in ATR mode.

Tensile Testing

Strength tests were performed in accordance with EN ISO 2062 at a jaw speed of 50 mm/min and a pre-stress of 0.05 MPa, with a jaw spacing of 12 cm. Three strength tests were performed on each prepared sample.

Results and Discussion

Determination of membrane thicknesses

The graph of membrane thickness test results for nanofiber membrane surfaces obtained with hemp additives is given in µm in Fig. 5 below. As can be seen in the graph, membrane thickness values increase significantly as the amount of hemp increases. While the thickness value of the PA66 nanofiber surface is 24 µm, this value increases to 37 µm for 10 H when the hemp content in the solution is increased.

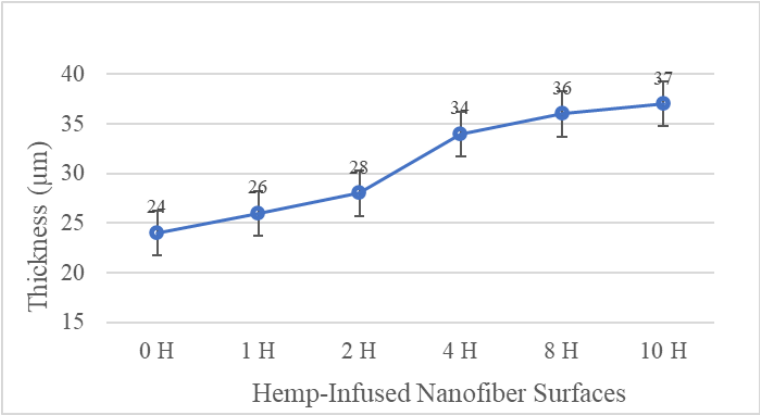

Fig. 5 The graph of membrane thickness test results

Differential Scanning Calorimetry (DSC)

DSC serves as a primary analytical method for investigating thermal characteristics in polymeric systems. The thermogram obtained from DSC analyses of nanofiber membrane samples produced by electrospinning using PA66 polymer solutions containing 10% hemp additives is shown in Fig. 6 below.

The thermograms obtained from DSC analyses of the produced PA66 nanofiber textile surface samples at a heating rate of 10°C/min revealed an endothermic peak around 251-258°C. Because the PA66 polymer has a thermoplastic structure, the DSC thermograms showed a melting endotherm. These endothermic peak temperatures represent the melting temperature of the produced PA66 nanofiber sample, and the results are consistent with and support the literature (Kayacı et al., 2015).

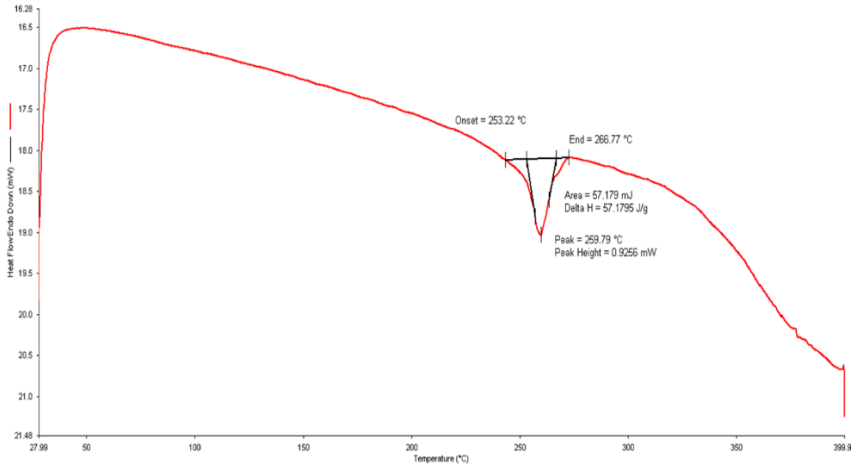

Fig. 6 DSC thermograms of PA66 polymer solutions containing 10% hemp additives

Thermogravimetric Analysis (TGA)

Figure 7 shows the TGA test graphs for 100% PA66 without hemp and 10% hemp-infused nanofiber samples.

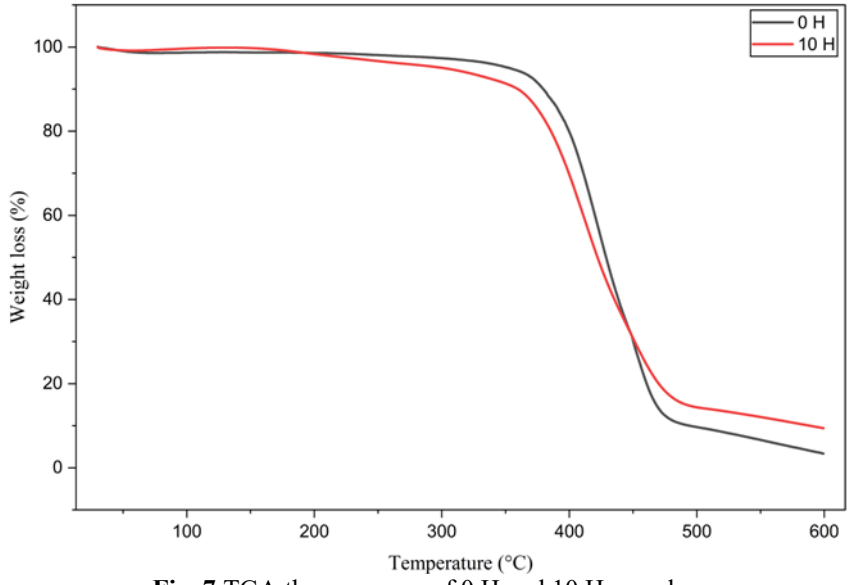

Fig. 7 TGA thermograms of 0 H and 10 H samples

The 100% PA66 sample showed a 97% mass loss at 600 °C without hemp, while the 10% hemp-infused nanofiber surfaces showed a 90% mass loss at 600 °C. TGA analyses of the 100% PA66 sample and the nanofibers obtained with a 10% hemp-infused ratio showed that, after an initial sharp decrease, the mass loss continued slowly and almost completely disintegrated. Consequently, it can be stated that hemp nanofibers are more durable at high temperatures than 100% PA66 polymer nanofibers. It can be stated that the structural stability of hemp-infused nanofiber materials increases with increasing temperature.

Fourier-transform Infrared Spectroscopy (FT-IR)

IR spectroscopy is one of the important techniques that provides information about the functional groups in a molecule. FTIR spectra of hemp-doped PA66 nanofiber membranes are shown in Fig. 8.

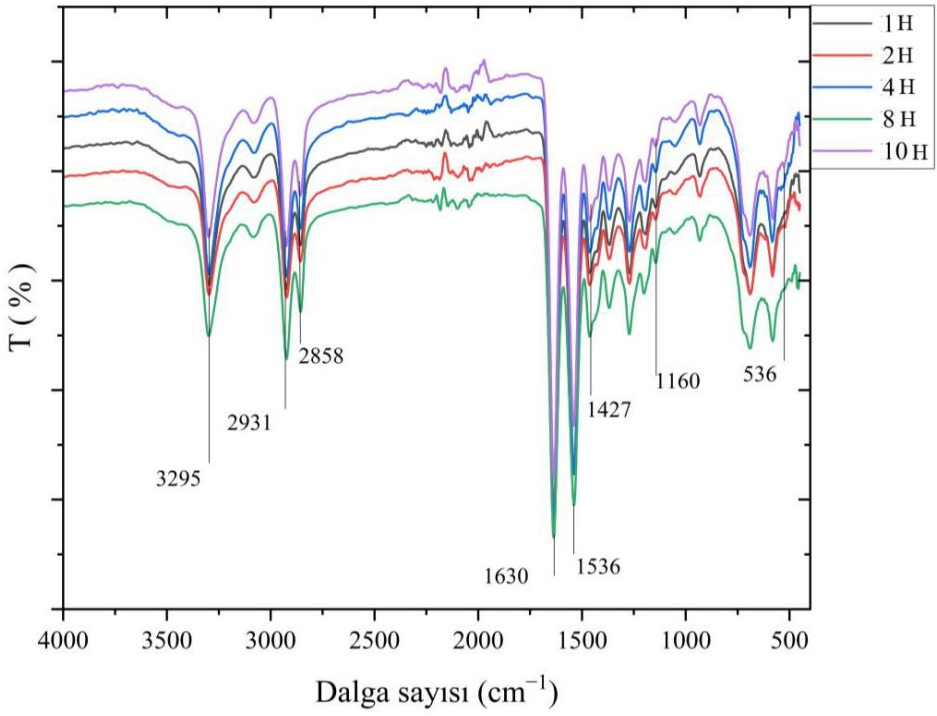

Fig. 8 FT-IR bands of stabilized hemp fibers and untreated

While the absorption peak belonging to the free N-H stretching between the polymer chains is expected to occur at wavenumbers above 3310 cm^{-1}, no absorption peak is observed in the spectrum at these wavenumbers. This can be explained by the fact that almost 100% of the N-H stretching in the structure is due to hydrogen bonds. The N-H and C=O stretching vibrations, which arise as a result of the interactions caused by the hydrogen bonds between the polymer

chains, were observed as absorption bands at 3295 and 1630 cm^{-1}, respectively. While asymmetric C-H stretching was observed at 2931 cm^{-1}, symmetric C-H stretching was observed at 2858 cm^{-1} (Tuncel, 2019). The peak observed at 1160 cm^{-1} reveals the presence of vibrations originating specifically from the cellulose structure. It is also clearly seen that the peak at 536 cm^{-1}, attributed to the characteristic O=C-N bending of PA66, disappears. This study demonstrates that a higher hemp doping ratio can be used to identify hemp functional groups, and a subsequent study can be hypothesized.

Tensile Properties

Tensile strength graphs obtained from the strength test results of hemp-reinforced PA66 nanofiber membranes are given in Fig. 9. The strength values of hemp-free PA66 nanofiber membranes were found to be higher than the strength values of other hemp-reinforced PA66 nanofiber membranes. The decrease in tensile strength values with increasing hemp additive ratios can be explained by the weakening of H-bonds between the polyamide chains in the structure. Furthermore, the weakening in the bond structure can be explained by the increase in the stiffness structure (Kuo et al., 2006). In addition, cellulosic hemp contains hydroxyl groups in its structure. Due to these groups in its structure, it can provide hardness and brittleness properties in materials (Zhou, 2015). In hemp-reinforced PA66 blends, hydrogen bonds in the structure are broken or weakened with increasing hemp ratio, while the formation of an amide plane in the -CO-N-H plane can be observed with the addition of hemp ratio. This study suggests that new hydrogen bonds are formed between the polyamide chains and cellulose molecules after the mixing process (Zhang, 2009). This can also lead to an increase in the fraction.

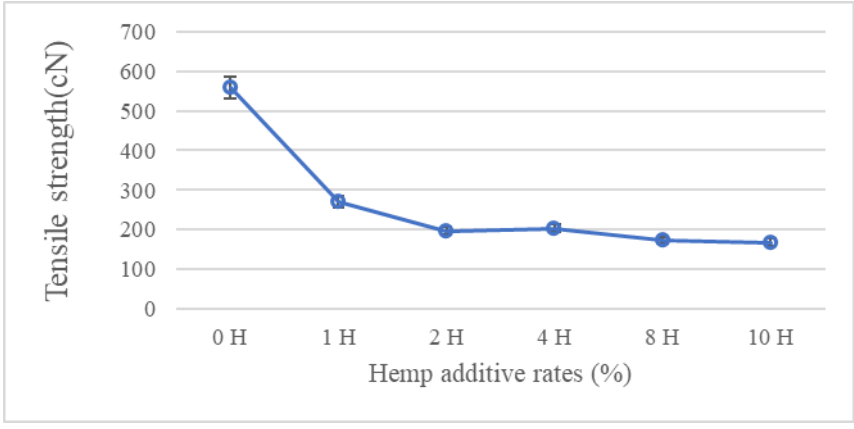

Fig. 9 Tensile strength graphs obtained from the strength test results of hemp-reinforced PA66 nanofiber membranes

Elongation graphs obtained from the strength test results of hemp-reinforced PA66 nanofiber membranes are given in Fig. 10.

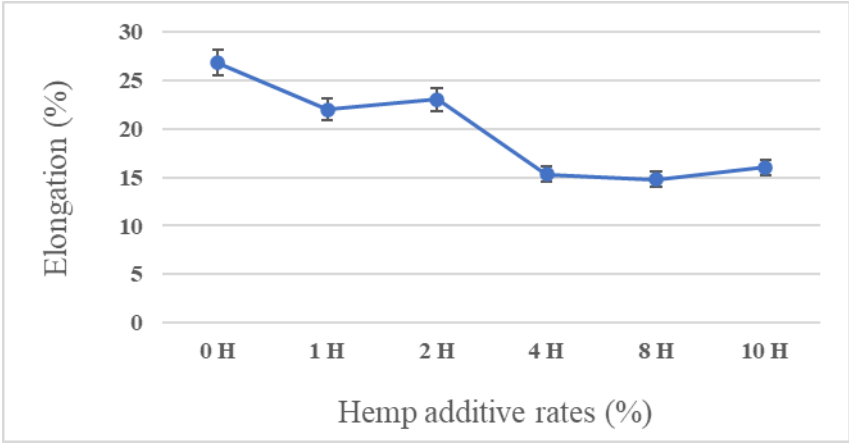

Fig. 10 Elongation graphs obtained from the strength test results of hemp-reinforced PA66 nanofiber membranes

Young Modulus graphs obtained from the strength test results of hemp-reinforced PA66 nanofiber membranes are given in Fig. 11.

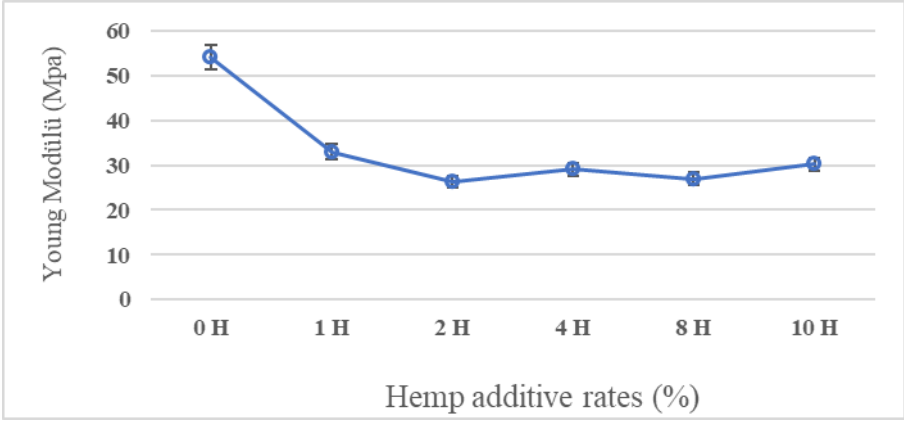

Fig. 11 Young Modulus graphs obtained from the strength test results of hemp-reinforced PA66 nanofiber membranes

Conclusions

In this study, membranes with nanofiber diameters were successfully obtained from hemp-reinforced PA66 polymer using electrospinning. Initially, hemp samples were ground using the ball milling technique. Hemp fibers were pretreated with alkali (7% NaOH at 120°C for half an hour) before milling. In

this study, 200 g hemp-reinforced PA66 solutions were prepared in a 3:1 formic acid-acetic acid organic solvent. PA66/Hemp (100/0, 99/1, 98/2, 96/4, 92/8, and 90/10) weight mixtures were obtained, respectively, to achieve a total solids content of 10% in the solution. Membrane thickness studies showed that as the amount of hemp increases, membrane thickness values also increase clearly. FTIR spectra revealed the vibration modes of the membrane samples with the resulting nanofiber structure, and it was observed that the vibration modes of the nanofibers produced with PA66 polymer and hemp additives were consistent with previous studies. C-O, antisymmetric and asymmetric axial stretching around 1300-1100 cm^{-1} and 1150-1000 cm^{-1}, respectively. The future of biodegradable membranes appears quite bright with the growing interest in environmental sustainability, circular economy, and green technologies. Especially with plastic pollution and microplastics on the global agenda, biodegradable (biodegradable) membranes are emerging as an environmentally friendly alternative to traditional synthetic polymers in many sectors. This study specifically focuses on characterization studies related to the reduced use of petroleum-based polymers. Therefore, based on scientific studies, we can say that the use of cellulose-based industrial hemp in nanofiber structures holds promise.

Acknowledgements

This study was supported by Yozgat Bozok University Scientific Research Projects with project code FKA-2023-1158.

References

Brown, T. (2020). Synthesis and properties of nylon 66. Materials Science Journal, 45(3), 123-134.

Dhondt, F. (2020). The future of hemp fibres under changing climate conditions (Doctoral dissertation, Hogeschool van Amsterdam).

Johnson, L. (2021). Chemical composition and properties of ABS. Advances in Polymer Science, 47(3), 345-360.

Ji A, Jia L, Kumar D, Yoo CG. Recent advancements in biological conversion of industrial hemp for biofuel and value-added products. Fermentation. 2021;7(1):6. https://doi.org/10.3390/fermentation7010006

Luo, C., Stoyanov, S., Stride, E., Pelan, E., & Edirisinghe, M. (2012). Electrospinning Versus Fibre Production Methods: From Specifics to Technological Convergence. Chem. Soc. Rev.,41(13): 4708–4735.

Lyons, J., Li, C., & Ko, F. (2004). Melt-Electrospinning Part I: Processing Parameters And Geometric Properties. Polymer, 45(22). 7597–7603.

Özdemir, E., (2001). "Polipropilen (PP) ve Naylon 66 (PA66) Plastiklerine Katılan Cam Elyafın Mekanik Özelliklere Etkisinin Deneysel İncelenmesi" Gazi Üniverstesi Fen Bilimleri Enstitüsi, Yüksek Lisans Tezi, Ankara, s.28.

Pakarinen, A., Zhang, J., Brock, T., Maijala, P., & Viikari, L. (2012). Enzymatic accessibility of fiber hemp is enhanced by enzymatic or chemical removal of pectin. Bioresource technology, 107, 275-281.

Rajeshbijwe, J., Tewari, U., ''Abrasive wear performance of various polyamides'', Wear, 252, 769–776, 2002.

Reddy, N., & Yang, Y. (2008). Characterizing natural cellulose fibers from velvet leaf (Abutilon theophrasti) stems. Bioresource Technology, 99(7), 2449-2454.

Smith, A. (2019). Overview of glass fiber: Characteristics and applications. Polymer Chemistry Today, 12(1), 67-89.

Subbiah, T., Bhat, G. S., Tock, R. W., Parameswaran, S., & Ramkumar, S. S. (2005). Electrospinning of Nanofibers. Journal of Applied Polymer Science, 96: 557–569.

Suwantong, O., Ruktanonchai, U., & Supaphol, P. (2008). Electrospun Cellulose Acetate Fiber Mats Containing Asiaticoside or Centella Asiatica Crude Extract And The Release Characteristics of Asiaticoside. Polymer, 49, 4239-4247

Taylor, R. (2020). Glass fiber in construction industry. Construction Materials Review, 39(3), 345-360.

Üstündağ, G. (2009). Elektrospinning Yöntemi ile Biyomedikal Kullanıma Yönelik Nanolif Yüzey Üretimi ve Uygulaması. Yüksek Lisans Tezi: Uludağ Üniversitesi Mühendislik Mimarlık Fakültesi Dergisi. 1 (14):159-172

Westerhuis, W., van Delden, S. H., van Dam, J. E. G., Marinho, J. P., Struik, P. C., & Stomph, T. J. (2019). Plant weight determines secondary fibre development in fibre hemp (Cannabis sativa L.). Industrial crops and products, 139, 111493.

Yıldırım, B. (2016). Polimer Esaslı Grafen Katkılı Yeni Nesil İletken Nanokompozit Malzemelerin Üretimi, Yapısal Özelliklerinin ve İletkenlik Karakteristiklerinin İncelenmesi. Yüksek Lisans: Kahramanmaraş Sütçü İmam Üniversitesi. Fen Bilimleri Enstitüsü. Kahramanmaraş.24

Zhang, X., Guo, J., Ma, Y., Lyu, L., Ji, Y., Guo, Y., & Hao, X. (2021). Green degumming technology of hemp and a comparison between chemical and biological degumming. ACS omega, 6(50), 35067-35075.

Zhao J, Xu Y, Wang W, Griffin J, Roozeboom, K. Bioconversion of industrial hemp biomass for bioethanol production: A review. Fuel. 2020;281(1):118725. https://doi.org/10.1016/j.fuel.2020.118725